Research Article

International Journal of Distributed Sensor Networks

International Journal of Distributed Sensor Networks
2017, Vol. 13(9)

DOI: 10.1177/1550147717729793
journals.sagepub.com/home/ijdsn
SAGE

Harmonic clutter recognition and suppression for automotive radar sensors

Jae-Eun Lee[1], Hae-Seung Lim[1], Seong-Hee Jeong[1], Hyun-Chool Shin[2], Seong-Wook Lee[3] and Seong-Cheol Kim[3]

Abstract

In this article, we propose a novel harmonic clutter recognition and suppression method to overcome the deterioration of a target- or vehicle-detection performance due to harmonic clutters. Although several studies have been performed on the reflection and diffraction on road surfaces for automotive radar sensors, most of them did not consider the case where metallic structures such as iron tunnels with greater reflection are densely distributed. The proposed method measures the periodicity of harmonic clutters by analyzing the spectral characteristics of the received radar signal with various road conditions. The proposed method can successfully recognize harmonic clutters. In addition, experimental results show that early detection of a target vehicle in an iron tunnel under adaptive cruise control is improved using the proposed clutter suppression method.

Keywords

Automotive radar, clutter recognition, clutter suppression, frequency-modulated continuous waves, harmonic clutter

Date received: 9 December 2016; accepted: 31 July 2017

Academic Editor: Kye-Shin Lee

Introduction

With the grooming demand for autonomous driving, there has been paid a great attention to the incorporation of multiple sensors.[1,2] The detection performance of the automotive radar looks outstanding compared to other sensors in poor weather conditions or poor environmental conditions of the roads. Among many applications of the automotive radar, the adaptive cruise control (ACC) and the autonomous emergency braking (AEB) using forward looking radars are the most basic functions for safety and convenience.[3–5] Using ACC and AEB functions, drivers can be guaranteed safety as well as convenience when visibility is poor under bad weather conditions. Nowadays, most of forward looking radars are multi-beam, multi-range (MBMR) radars which consist of integrated narrow long-range beam and wide short-range beam in a single radar sensor.[6] The installation rate of automotive radars worldwide will increase because of its low cost and small size by employing MBMR radar. As the signal quality of automotive radars decreases by downsizing, their detection performance should be maintained for the safety. Moreover, their detection performance can be deteriorated by man-made structures on roads such as iron tunnels (ITs), guardrails (GRs), or soundproof (SP) walls that have high reflectivity for electromagnetic waves and generate harmonic clutters which

[1]Mando Corporation, Seongnam, Korea
[2]School of Electronic Engineering, Soongsil University, Seoul, Korea
[3]Department of Electrical and Computer Engineering and INMC, Seoul National University, Seoul, Korea

Corresponding author:
Seong-Cheol Kim, Department of Electrical and Computer Engineering and INMC, Seoul National University, Seoul 08826, Korea.
Email: sckim@maxwell.snu.ac.kr

are due to periodic structures on roads. To overcome the limitation of radar hardware, we need to implement a signal-processing technique to improve the detection performance.

There have been several studies about reflection or diffraction on road surfaces.[7–9] These studies have found that the detection performance of radars is dependent on the surface roughness and road slopes. Meanwhile, there have been few studies on clutters caused by man-made structures on roads.[10,11] These studies focused on ultra wideband pulse radars, so their application to frequency-modulated continuous waves (FMCW)[12–14] is not appropriate. In addition, there have been several approaches to discriminate over-head or neighboring structures from stationary targets on roads.[15–17] A recent study has introduced a recognition method for ITs that influence the detection performance of radars because of large reflections.[18] However, few of them considered the suppression method to improve the detection performance despite clutters on roads.

In this article, we propose a novel harmonic clutter recognition and suppression method to overcome the deterioration of detection performance due to harmonic clutters. The proposed method recognizes harmonic clutters by analyzing the spectrum of the received signal under different road conditions. We observed that the spectrum contains equally spaced frequency peaks which are harmonic clutters due to periodic structures such as ITs, GRs, and SP walls. The proposed recognition method measures the level of clutters by applying the discrete Fourier transform (DFT) to the spectrum in frequency domain and incorporating the concept of the peak-to-average power ratio (PAPR). The proposed suppression method restrains harmonic clutters by reducing the level of clutters. Raw experimental data were obtained using a 77-GHz forward looking FMCW radar for the ACC and AEB. We demonstrate that the proposed method can successfully recognize and suppress harmonic clutters using real field data. In addition, the detection results show that the problem of the late detection of a target vehicle in an IT under ACC is improved using the proposed clutter suppression method.

This article is organized as follows. In section "Clutter recognition," we present a description of the radar model and the spectral analysis of the received signal in accordance with various road environments. Then, we discuss in detail the proposed harmonic clutter recognition method. In section "Clutter suppression," we present and verify the proposed suppression method by performing the software-in-the-loop (SIL) test using real data obtained from the radar. In section "Experimental results," we show the experimental results of the improved early detection in the ACC performance, and in "Conclusion," we summarize and conclude this article.

Clutter recognition

In this section, we present a mathematical description of a signal model received from the radar. Then, we repeat the spectral analysis and harmonic analysis of the radar signal under various road conditions. We propose a novel method to recognize harmonic clutters based on the harmonic characteristics of periodic structures.

Radar model

In this study, we employed a 77-GHz forward looking radar of Mando Corporation using FMCW modulation. If the transmitted signal of the FMCW radar is reflected by L targets, the discrete-time received signal can be defined as

$$\begin{aligned} x(n) &= s(n) + \nu(n) \\ &= \sum_{i=0}^{L-1} A(i)\cos(2\pi f(i)n + \phi(i)) + \nu(n) \end{aligned} \tag{1}$$

where $n(0 \le n < N)$ is the discrete-time index of the received signal during a single *scan* (which is the time unit of radar signal processing), and N is the number of samples in a single *scan*. $\nu(n)$ consists of noise components and undesired clutter signals. $A(i)$ is the amplitude of the reflected signal from each target, and $\phi(i)$ is the phase component of the received signals from each target. $f(i)$ is composed of $f_r(i)$ (which is the frequency difference due to the distance of the target and the radar) and $f_d(i)$ (which depends on the relative velocity between the radar and the target). $f_r(i)$ and $f_d(i)$ can be, respectively, obtained as follows

$$f_r(i) = \frac{2B}{cT}R(i) \tag{2}$$

and

$$f_d(i) = \frac{2f_0}{c}V_r(i) = \frac{2}{\lambda}V_r(i) \tag{3}$$

where B is the bandwidth, T is the duration of frequency chirping, c is the speed of light, f_0 indicates the center frequency, and $R(i)$ and $V_r(i)$ are the distance and relative velocity between the radar and each target, respectively.

Then, the frequency domain signals that were calculated using the short-time Fourier transform (STFT) can be represented as

$$X(f, m) = STFT(x(m)) \tag{4}$$

where f is the frequency index, m is the *scan* index, and $x(m) = [x((m-1)\cdot N), x(1 + (m-1)\cdot N), \ldots, x(N - 1 + (m-1)\cdot N)]$.

Spectral analysis of road environment

To analyze the characteristics of the radar signal affected by clutters on the road, we compared its spectral characteristics. To extract the characteristics of clutters that adversely affect the radar, we examined the frequency characteristics using the signal acquired on a normal road, an expressway, a SP wall, a GR, and the entry to and inside ITs. In the previous study,[18] we observed the spectrum spreading in dense structures such as ITs, SP walls, and GRs. More interestingly, we discovered the presence of spectral harmonics in the magnitude response under such environments. To extract the harmonics, we conducted DFT on the magnitude response of the spectrum ($X(f, m)$), as follows

$$H(h, m) = \sum_{f=0}^{N-1} |X(f, m)| e^{-j\frac{2\pi h}{N} f} \tag{5}$$

we call $|H(h, m)|$ a *harmonogram*.

Figure 1 illustrates spectral harmonics under a normal road, an IT, and a GR. The results under each road environment consist of five subfigures: the captured image on roads, the whole spectrogram, the spectrum at a certain time instance marked as the vertical solid line, the harmonogram in equation (5) at the same instance in time, and the whole harmonogram.

The spectrogram ($|X(f, m)|$) in Figure 1(a) shows high intensity in the low-frequency band under the normal road conditions, which indicates that a single target with a velocity that is similar to that of the own vehicle exists at the front. Other diagonal lines indicate targets have velocities that differ from that of the own vehicle, or stationary objects such as streetlights or road signs. The spectrum ($|X(f, m = 30)|$) shows the time instance ($m = 30$) marked as the vertical solid line at the spectrogram. This includes a frequency peak with high magnitude that corresponds to the target and low peaks from other targets. If we conduct another Fourier transform to the spectrum, we can obtain the harmonogram ($|H(h, m = 30)|$) at the same time instance in Figure 1(a), which is symmetric because the magnitude response is real-valued. There are no notable components, and it has a flat floor. The whole harmonogram ($|H(h, m)|$) shows that there are no prominent components during the measurement time.

Figure 1(b) demonstrates the situation inside the IT. The high-intensity response is spread over the entire band because of iron structures inside the tunnel in the spectrogram ($|X(f, m)|$); the spectrum ($|X(f, m = 30)|$) exhibits periodicity in the frequency domain, and the harmonogram ($|H(f, m = 30)|$) at the time instance ($m = 30$) shows several harmonics, which represent harmonic clutters from the periodic structures. The IT consists of periodic structures that are equally spaced, so the periodic components are concentrated in harmonic peaks in the harmonogram ($|H(h, m)|$). Other signals are spread onto the floor because targets do not exist periodically like man-made structures in an IT. We confirmed that there are prominent harmonics during the measurement in the harmonogram, and these appear as horizontal lines.

Figure 1(c) shows the condition involving a GR on the road. The high-intensity response shows up in the spectrogram ($|X(f, m)|$) as the own vehicle meets a GR. The frequency peaks in the spectrum ($|X(f, m = 70)|$) are densely distributed, and the harmonogram at the time instance ($m = 70$) shows prominent peaks that correspond to the periodic structures on GRs. In the whole harmonogram, we confirmed that harmonics appear in the middle of the measurement as the own vehicle meets GRs. Generally, ITs and GRs contain iron structures that have almost the same spacing. The peak components represent the periodic structures, which appear as harmonic clutters to the received radar signal. Many man-made structures with high reflectivity such as ITs, GRs, and SP walls consist of evenly spaced structures. Thus, if the periodicity in the spectrum can be measured, we can recognize clutters that cause harmful effects to the radar on the road.

Proposed clutter recognition method (measuring harmonics of clutters)

To recognize clutters that deteriorate the detection performance of the radar, we need a quantitative measure that can be uniformly applied. The harmonogram reveals distinct harmonic characteristics. Therefore, harmonic clutters can be recognized if we can extract the peak components from the harmonogram. Considering the PAPR in the harmonogram, we defined the level of harmonic clutters, L_C, using the harmonogram as follows

$$L_C(m) = \frac{max(|H(h, m)|)^2}{|H(h, m)|^2_{mean}}. \tag{6}$$

We can calculate the average value, $|H(h, m)|^2_{mean}$, with the exception of peak components that designate guard cells which are adjacent cells to the peak. A majority of peak components consist of harmonic clutters, and we therefore eliminate peak components when calculating the average value to obtain a more precise value of the floor level. To verify the validity of the proposed method, we applied the proposed method to real data from a normal road, an IT, and a GR as shown in Figure 2. Figure 2(a) shows the spectrogram of the received signal and the harmonogram on a normal public road. We cannot find periodic components from the spectrogram and harmonogram, and the level of harmonic clutter, L_C, is stable with a low value. Figure 2(b) also shows the spectrogram and

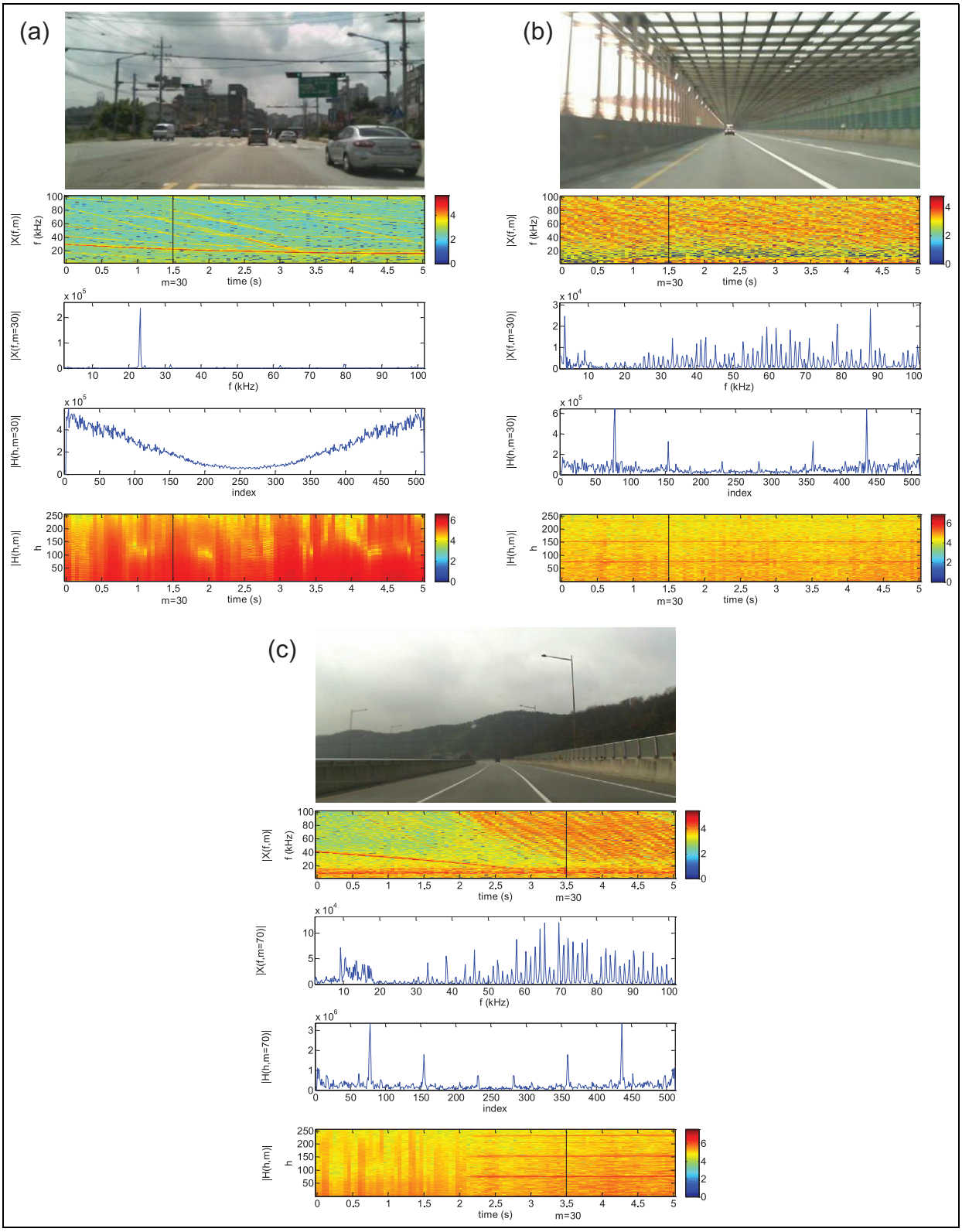

Figure 1. Spectrograms and harmonograms of the received radar signals under various road conditions: (a) normal road, (b) iron tunnel, and (c) guardrail.

harmonogram at the entry of an IT. We can confirm that horizontal lines appear around the entrance of the tunnel, which indicate the presence of harmonic clutters. The proposed level of harmonic clutters increases as the own vehicle approaches the IT. Figure 2(c) shows a similar tendency as in Figure 2(b) under

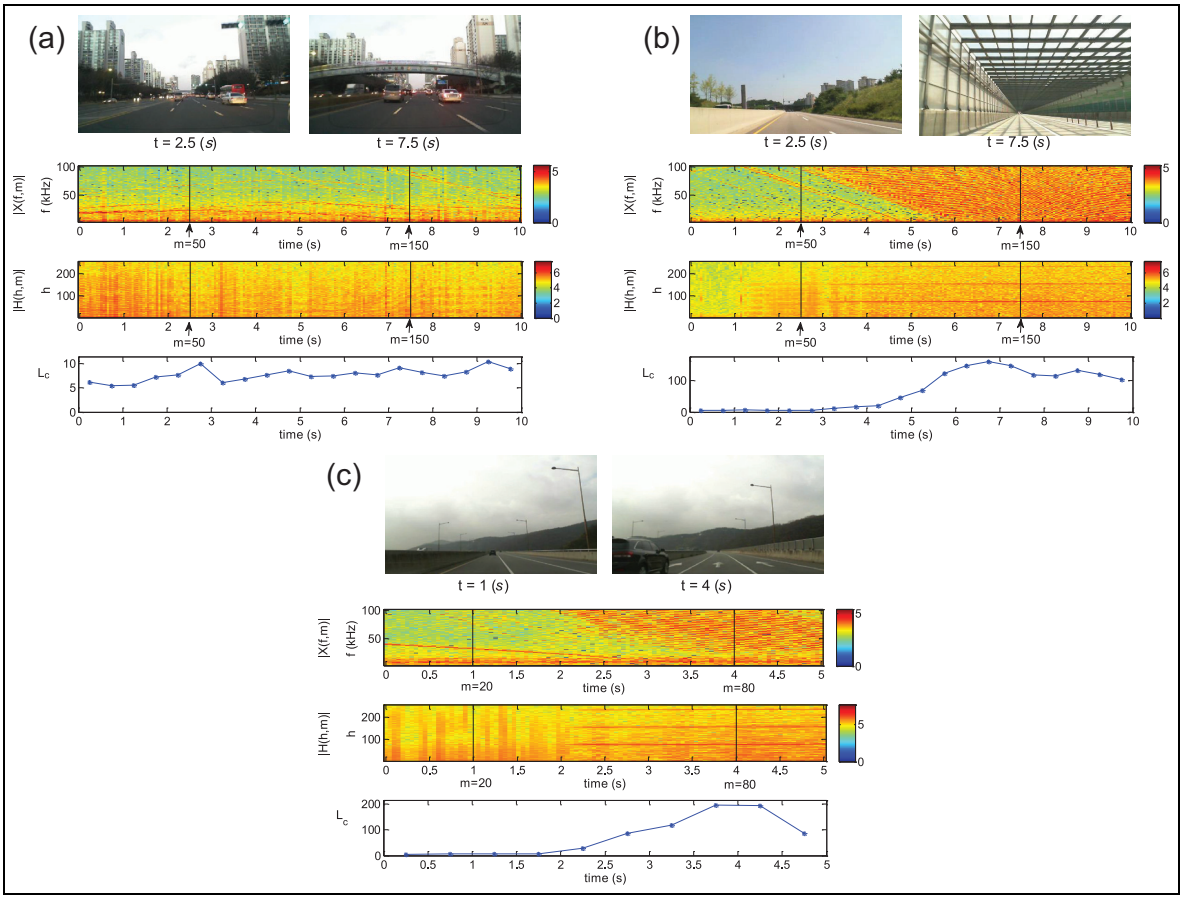

Figure 2. Analysis of the level of harmonic clutters under various road conditions: (a) normal road, (b) iron tunnel, and (c) guardrail.

the situation of a GR. We can confirm that the proposed method validates the stable recognition of harmonic clutters caused by periodic structures.

Clutter suppression

In this section, we propose an efficient clutter suppression method, and we evaluate the performance of the proposed method using real data acquired from the radar.

Proposed clutter suppression method

The conventional iron-tunnel recognition method has a limitation in terms of its ability to improve the detection performance of the radar because it controls only the parameters for signal processing, such as the threshold for extraction of target peaks or parameters of tracking algorithm. Furthermore, it does not deal with the clutter signals. In this case, there is an increased probability of occurring false alarm. Thus, it can increase the signal processing required after frequency peak extraction, including the tracking algorithm to prevent false alarm.

To reduce this risk, we propose a new approach to suppress harmonic clutters maintaining signals from targets. If harmonic clutters can be recognized using the proposed method, we can reduce clutters by suppressing the peak components of the magnitude response from the DFT ($|H(h,m)|$). Harmonic peaks contain concentrated clutter signals and spread target signals. The loss of information from targets is negligible because the components of clutter signals are much higher than those of target signals. We can extract the harmonic peaks in the magnitude response of $|H(h,m)|$ by simply using the cell-averaging constant false alarm rate (CA-CFAR) algorithm.[19]

If the presence of clutters is recognized from the recognition method, we calculate the average value of the magnitude of reference cells which are included in a window under the test around each peak from the CA-CFAR algorithm, with the exception of guard cells. Then, we set the magnitude value of guard cells, including the peak cell, as the average of the reference cells maintaining the phase of each cell as follows

$$\overline{H(h,m)} = \begin{cases} A_r(k)e^{j\phi(h)}, \\ h_{p(k)} - \frac{N_g}{2} \le h \le h_{p(k)} + \frac{N_g}{2} \\ \text{if } L_C(m) > L_{th} \\ H(h,m), \quad \text{otherwise} \end{cases} \tag{7}$$

where $\overline{H(h,m)}$ is the harmonic clutter–suppressed harmonogram, $A_r(k)$ is the average magnitude of reference

cells, $\phi(h)$ is the phase component of $H(h, m)$, $h_{p(k)}$ represents the index of the kth peak, N_g is the number of guard cells, and L_{th} is the threshold of the level of harmonic clutter for recognition which is calculated as three times of mean power of harmonogram at normal road condition. To better understand the usefulness of the proposed method, we conducted harmonic clutter suppression using data obtained in an IT at an instance in time when the target was not extracted as in Figure 3. The first figure is the spectrogram, and the vertical solid line indicates the instance in time, which we investigated to compare the effect of the proposed

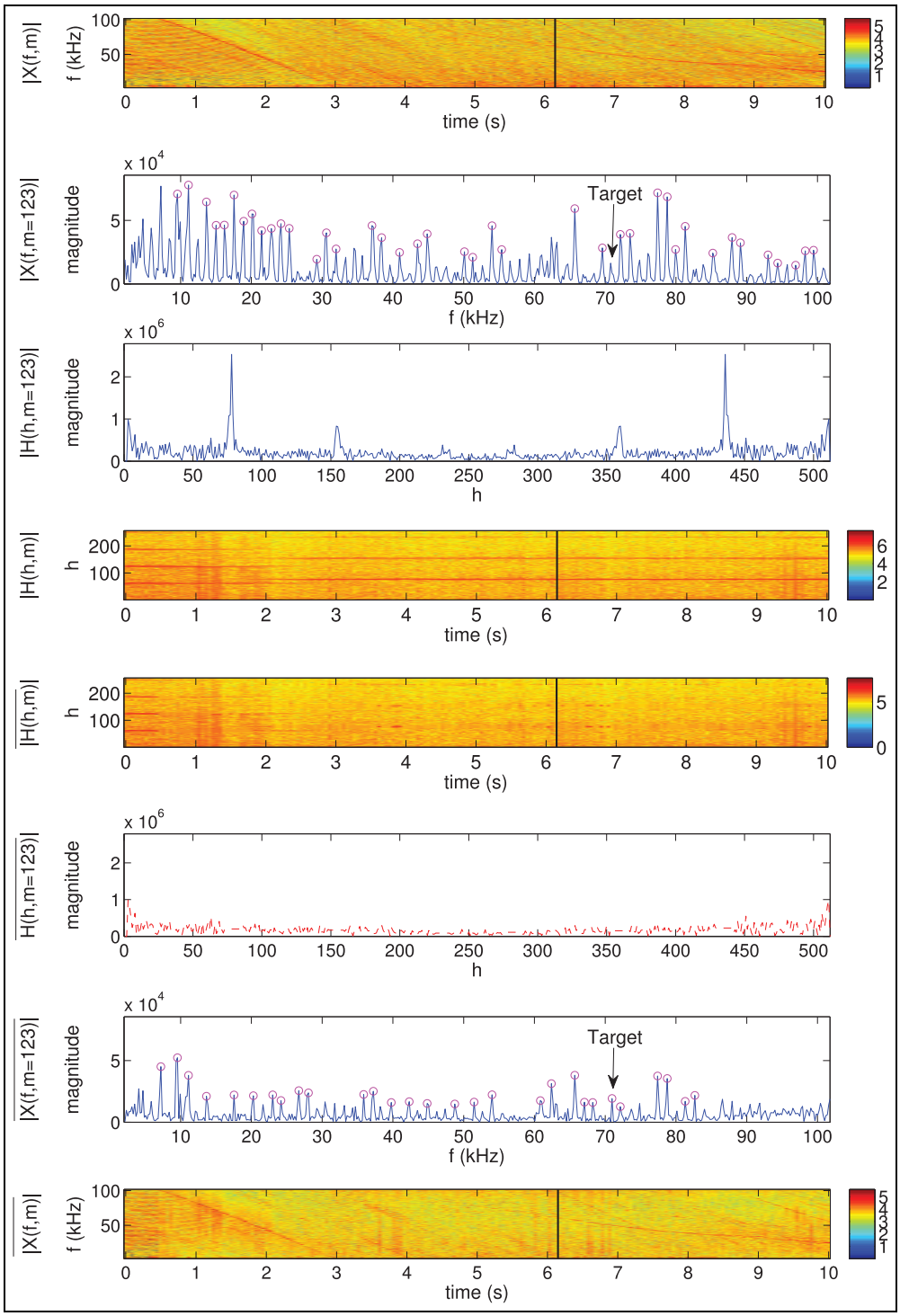

Figure 3. An example of clutter suppression results in an iron tunnel.

Table 1. Profile of various harmonic clutters and the level of harmonic clutters.

Case	Type	Date of experiment	Geographic coordinate (latitude, longitude)	Time (s)		$10\log_{10}(L_C)$ (dB)		CSR (%)
				Entry	Exit	Without	With	
A	IT	16 November 2015	(32.27, 127.08)	–	4.75	20.79	4.69	77.4
B	IT	18 August 2015	(32.17, 127.03)	5.75	–	21.08	4.74	77.5
C	IT	11 August 2015	(32.27, 127.08)	6.25	17.75	19.35	4.94	77.5
D	IT	2 January 2016	(36.47, 127.25)	10.75	–	20.36	4.59	77.5
E	IT	2 January 2016	(36.47, 127.25)	–	15.25	19.49	5.19	73.4
F	IT	13 August 2015	(32.17, 127.03)	3.25	–	21.16	4.71	77.7
G	GR	20 November 2015	(32.27, 127.08)	3.25	–	21.71	4.89	77.5
H	GR	18 August 2015	(32.27, 127.08)	6.25	–	13.73	5.12	62.7
I	SP	16 November 2015	(32.27, 127.08)	5.25	–	19.96	4.94	75.3

CSR: clutter suppression ratio; IT: iron tunnel; GR: guardrail; SP: soundproof.

clutter suppression method. The next figure is the spectrum of the received signal in an IT, where there is a target vehicle in front of the own vehicle. The next figure shows the harmonogram in the same time instance of the spectrum. We can confirm that several peaks from harmonic clutters, which are due to periodic structures, and the rest of the signal floor are as results of the targets. The clutters appear as periodic signals, so the clutters are compressed by the DFT and concentrated into harmonic peaks. The fourth figure represents the whole harmonogram, and the next figure is the harmonic clutter–suppressed harmonogram ($|\overline{H(h,m)}|$). The dashed line in the sixth figure represents the suppressed harmonogram in a certain time instance ($|\overline{H(h,m=123)}|$). The next figure is the harmonic clutter–suppressed spectrum which denotes the magnitude of the result of inverse discrete Fourier transform (IDFT) of the previous peak-suppressed signal. Although the entire signal level is reduced, the decrease in the signal from the target is negligible because the majority of the suppressed peaks are from harmonic clutters. We can confirm that the signal from the target vehicle is obtained by conventional signal-processing algorithm. The final figure indicates the harmonic clutter–suppressed spectrogram ($|\overline{X(f,m)}|$). The overall intensity is decreased, and the diagonal lines in the spectrum are particularly suppressed.

Verification using real data

To verify that harmonic clutters can be recognized and suppressed using the proposed method, we tested the proposed method using acquired data in various road environments that contain harmonic clutters. Table 1 summarizes the types of harmonic clutters for which we conducted experiments, the dates of the experiment, the latitudinal and longitudinal coordinates of the clutters, the entry time and exit time, the average level of clutters in dB scale where there are harmonic clutters without and with clutter suppression, and the clutter suppression ratio (CSR) by calculating the difference of average level of clutters according to suppression as

$$CSR = \frac{10\log_{10}(L_{c,without}) - 10\log_{10}(L_{c,with})}{10\log_{10}(L_{c,without})} \times 100 \quad (8)$$

where $L_{c,without}$ and $L_{c,with}$ represent the average value of the level of clutters without and with suppression, respectively. The types of harmonic cutters contain an IT, a GR, and a SP wall.

We confirmed that there are significant differences between the average values of the level of harmonic clutters, L_C, without and with the clutter suppression. Figure 4(a) shows the effect of clutter suppression around the exit point of an IT. The first figure is the spectrogram of the received signal. The second and third figures represent the harmonogram containing clear horizontal lines, which are due to concentrated harmonic clutters, and the level of harmonic clutters, which has a high value before the exit point. The fourth and fifth figures show the harmonogram and the level of harmonic clutters after harmonic clutter suppression. We confirmed that horizontal lines are removed after the suppression, and the level of clutters remains stable from the beginning to the end of data. The final figure represents the harmonic clutter–suppressed spectrogram.

Figure 4(b) shows the location around the entry point of an IT. Similarly, we observe horizontal lines in the second figure and a high L_C after the entry point without the suppression. The harmonic clutter–suppressed harmonogram ($\overline{H(h,m)}$), L_C, and the harmonic clutter–suppressed spectrum ($\overline{X(f,m)}$) indicate the effect of the proposed harmonic clutter suppression method clearly.

Figure 4(c) shows a similar tendency as Figure 4(b) around a GR on the curved road. The intensity at high frequency is stronger than low frequency because the reflected signals from close GRs laid on the edge of roads are weak. However, reflected signals from long distances can be strong enough to disrupt the signals from a target in front of the own vehicle. Moreover, the probabilities of those effects can be increased on curved roads because reflections are higher than on the straight roads. The results

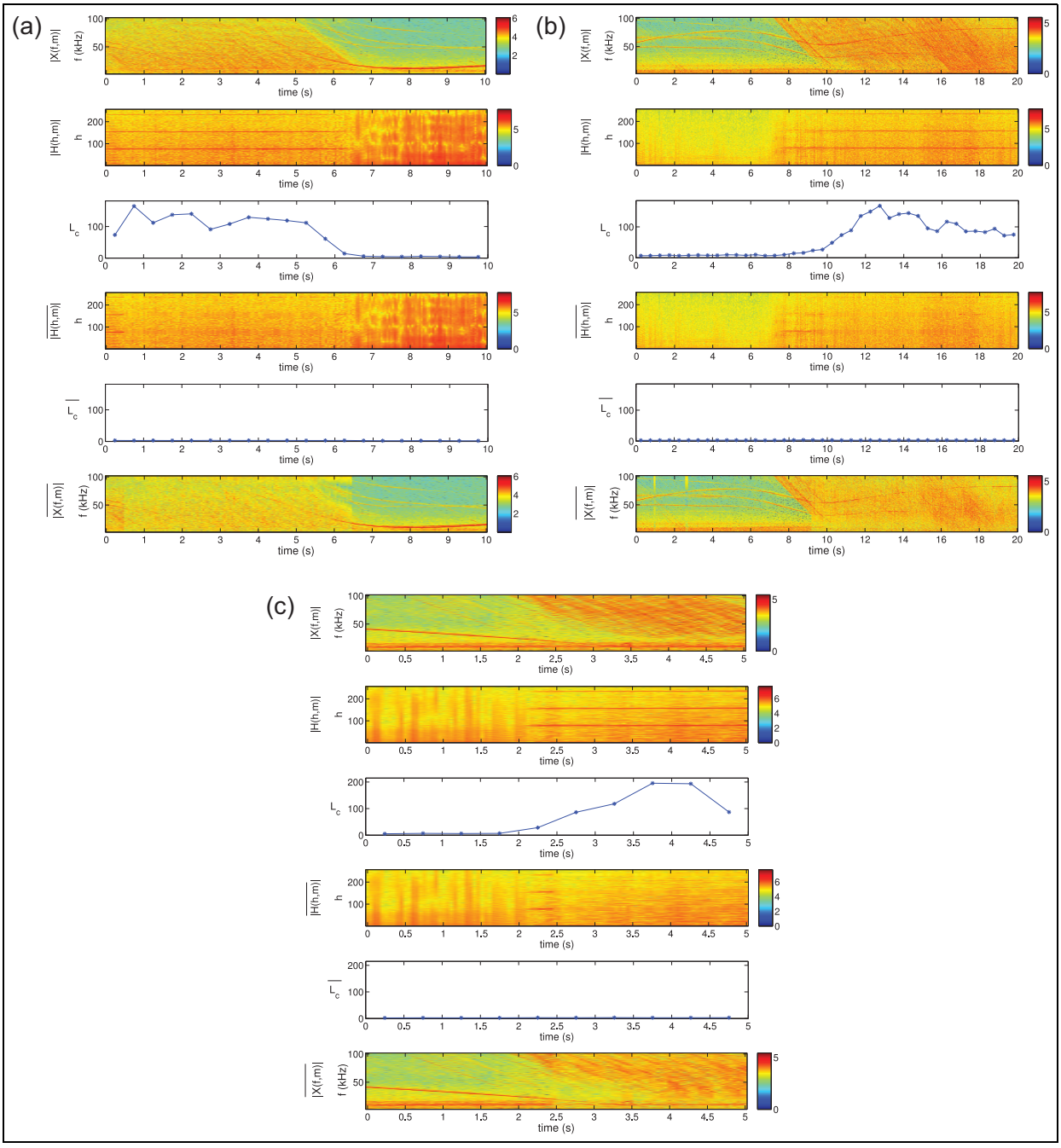

Figure 4. Results of harmonic clutter suppression: (a) case A (CSR = 77.4%), (b) case D (CSR = 77.5%), and (c) case G (CSR = 77.5%).

obtained for harmonic clutter suppression are similar to those of previous cases.

Experimental results

To determine the usefulness of the proposed harmonic clutter suppression method for ACC, we performed an experiment without the proposed method, and we gathered raw data from the radar. The bandwidth (B) of the transmitted signal is 500 MHz, and the chirp duration (T) is 5 ms with the center frequency (f_c) at 76.5 GHz. We conducted an SIL test using the same data to compare how quickly targets or vehicles are detected in the lane of the own vehicle with and without the proposed method inside an IT. We set the vehicle speed to ACC = 180 km/h, and the own vehicle was accelerated because of the absence of a target vehicle in the maximum detection range at the front. Then, the

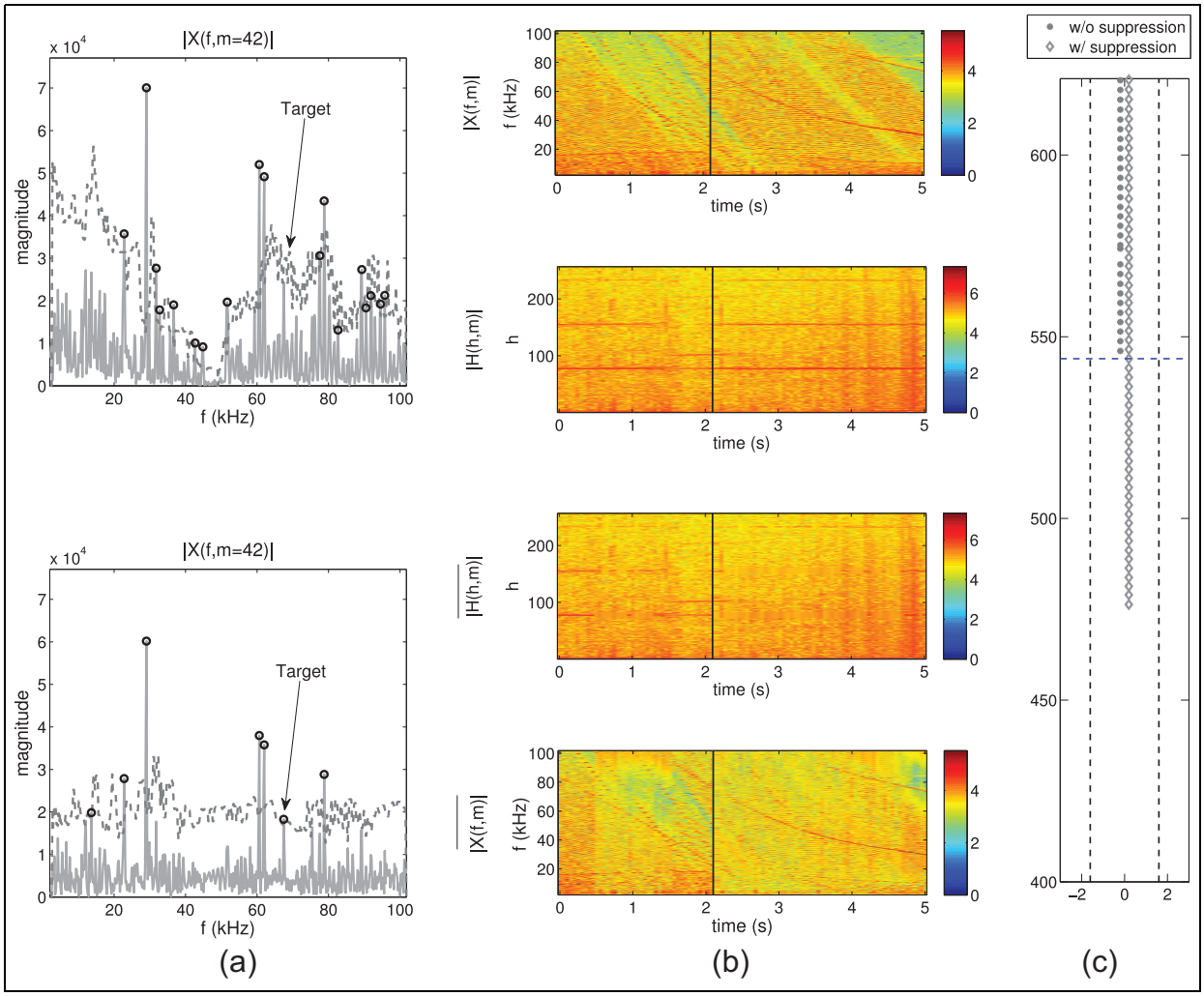

Figure 5. Comparison of detection results (early detection): (a) spectrum comparison, (b) comparison of spectrograms and harmonograms, and (c) trajectory comparison of detection results.

accelerating own vehicle performed sudden deceleration because of the late detection of the target vehicle. This situation could be dangerous if the distance between the own vehicle and the following vehicle is close.

Figure 5 shows the detection results with and without application of the harmonic clutter suppression method during the detection of the forward target vehicle inside the IT. Figure 5(a) show the spectrum comparison at the instance of time just before the target vehicle is detected by the radar of the own vehicle, and this is represented as the horizontal dashed line in Figure 5(c). The first spectrum represents the original spectrum obtained in the field experiment. There are many high-intensity harmonic clutters, so the target vehicle cannot be extracted because of the high clutter level. We confirmed that the spectrum after harmonic clutter suppression contains fewer clutter signals, whereas remaining information of targets. The frequency peak of the vehicle in front of the own vehicle can be obtained using the conventional CFAR algorithm.

Figure 5(b) shows spectrograms and harmonograms without and with the proposed method, respectively. The spectrogram and harmonogram without clutter suppression contain many clutter signals. However, we can confirm that horizontal lines by harmonic peaks are removed in the harmonogram, and diagonal lines with high intensity in the spectrogram are eliminated when we apply the proposed method.

Figure 5(c) shows the trajectory of the detected target vehicle along the distance axis. We can confirm that when harmonic clutters are suppressed using the proposed method, the target vehicle can be detected at an earlier time. The initial detection time is a critical factor in determining the performance of the ACC. The speed of the own vehicle was 170.6 km/h because of the continuous acceleration until the detection of the target vehicle in front of it, and the distance between the target

vehicle and the own vehicle was 104.1 m when the target vehicle was initially detected. The driver in the own vehicle had to make a sudden deceleration to avoid a collision. However, the distance between the target vehicle and the own vehicle was 169.85 m after harmonic clutter suppression. In this case, there is no need to make an abrupt deceleration, and there was sufficient time to comfortably control the own vehicle.

Conclusion

In this article, we proposed new approaches for the detection and suppression of harmonic clutters on roads using an automotive radar. We performed spectral and harmonic analyses of the radar signal received in various road conditions using a conventional spectrogram and suggested harmonogram. We then obtained the features under harmonic clutters using those analysis results. We proposed a level of harmonic clutters using the PAPR concept with a harmonogram to measure the characteristics of harmonic clutters quantitatively. We also proposed the suppression method of harmonic clutters by reducing the level of clutters of the spectrum. We performed experiments to verify that the proposed level of the clutter-based method is very useful for recognizing and suppressing harmonic clutters. In addition, the proposed harmonic clutter recognition and suppression method improved the performance and robustness of an ACC system where there were severe harmonic clutters which reduced detection performance of the radar. Although we performed the proposed method using several sets of real data acquired from public roads, more field tests may be needed to enable a statistical analysis of the proposed methods.

Declaration of conflicting interests

The author(s) declared no potential conflicts of interest with respect to the research, authorship, and/or publication of this article.

Funding

The author(s) disclosed receipt of the following financial support for the research, authorship, and/or publication of this article: This work was supported by the Technology Innovation Program (or Industrial Strategic technology development program, no. 10051134, Middle range radar (150 m) development for Euro NCAP AEB) funded By the Ministry of Trade, Industry and Energy (MI, Korea).

References

1. Okuda R, Kajiwara T and Terashima K. A survey of technical trend of ADAS and autonomous driving. In: *Proceedings of the technical program—international symposium on VLSI technology, systems and application (VLSI-TSA)*, Hsinchu, Taiwan, 28–30 April 2014, pp.1–4. New York: IEEE.
2. Dickmann J, Klappstein J, Hahn M, et al. Automotive radar the key technology for autonomous driving: from detection and ranging to environmental understanding. In: *Proceedings of the 2016 IEEE radar conference*, Philadelphia, PA, 2–6 May 2016, pp.1–6. New York: IEEE.
3. Coelingh E, Eidehall A and Bengtsson M. Collision warning with full auto brake and pedestrian detection—a practical example of automatic emergency braking. In: *Proceedings of the 13th international IEEE conference on intelligent transportation systems*, Funchal, 19–22 September 2010, pp.155–160. New York: IEEE.
4. Kopetz H and Poledna S. Autonomous emergency braking: a system-of-systems perspective. In: *Proceedings of the IEEE/IFIP conference on dependable systems and networks workshop*, Budapest, 24–27 June 2013, pp.1–7. New York: IEEE.
5. Vahidi A and Eskandarian A. Research advances in intelligent collision avoidance and adaptive cruise control. *IEEE T Intell Transp* 2003; 4(3): 143–153.
6. Jeong S, Yu H, Lee J, et al. A multi-beam and multi-range radar with FMCW and digital beam forming for automotive applications. *Prog Electromagn Res* 2012; 124: 285–299.
7. Nagy L. Electromagnetic reflectivity characteristics of road surfaces. *IEEE T Veh Technol* 1974; 23(4): 117–124.
8. Schneider R, Didascalou D and Wiesbeck W. Impact of road surfaces on millimeter-wave propagation. *IEEE T Veh Technol* 2000; 49(4): 1314–1320.
9. Pathak P, Burnside W and Marhefka R. A uniform GTD analysis of the diffraction of electromagnetic waves by a smooth convex surface. *IEEE T Antenn Propag* 1980; 28(5): 631–642.
10. Bouvier C, Martinet L, Favier G, et al. Radar clutter classification using autoregressive modelling, K-distribution and neural network. In: *Proceedings of the IEEE international conference on acoustics, speech, and signal processing*, Detroit, MI, 9–12 May 1995, vol. 3, pp.1820–1823. New York: IEEE.
11. Matsunami I and Kajiwara A. Clutter suppression scheme for vehicle radar. In: *Proceedings of the 2010 IEEE radio and wireless symposium (RWS)*, New Orleans, LA, 10–14 January 2010, pp.320–323. New York: IEEE.
12. Stove A. Linear FMCW radar techniques. *IEE Proc: F* 1992; 139(5): 343–350.
13. Skolnik M. *Introduction to radar systems*. New York: McGraw-Hill Book Company, 2001.
14. Barton D. *Radar system analysis and modeling*. Norwood, MA: Artech House, 2004.
15. Lundquist C and Schön T. Tracking stationary extended objects for road mapping using radar measurements. In: *Proceedings of the 2009 IEEE intelligent vehicles symposium*, Xi'an, China, 3–5 June 2009, pp.405–410. New York: IEEE.
16. Diewald F, Klappstein J, Sarholz F, et al. Radar-interference-based bridge identification for collision avoidance systems. In: *Proceedings of the 2011 IEEE intelligent*

vehicles symposium, Baden-Baden, 5–9 June 2011, pp.113–118. New York: IEEE.

17. Choi K, Seo G, Lee J, et al. Automatic radar horizontal alignment scheme using stationary target on public road. In: *Proceedings of the 2013 European microwave conference (EuMC)*, Nuremberg, 6–10 October 2013, pp.551–554. New York: IEEE.
18. Lee J, Lim H, Jeong S, et al. Enhanced iron-tunnel recognition for automotive radars. *IEEE T Veh Technol* 2016; 65(6): 4412–4418.
19. Rohling H. Radar CFAR thresholding in clutter and multiple target situations. *IEEE T Aero Elec Sys* 1983; 19(4): 608–621.